Low-threshold room-temperature AlGaAs/GaAs nanowire/single-quantum-well heterostructure laser

Xin Yan, Wei Wei, Fengling Tang, Xi Wang, Luying Li, Xia Zhang, and Xiaomin Ren

Citation: Appl. Phys. Lett. **110**, 061104 (2017); doi: 10.1063/1.4975780
View online: http://dx.doi.org/10.1063/1.4975780
View Table of Contents: http://aip.scitation.org/toc/apl/110/6
Published by the American Institute of Physics

Low-threshold room-temperature AlGaAs/GaAs nanowire/single-quantum-well heterostructure laser

Xin Yan,[1,a)] Wei Wei,[2,3,a)] Fengling Tang,[1] Xi Wang,[4] Luying Li,[4] Xia Zhang,[1,b)] and Xiaomin Ren[1]

[1]*State Key Laboratory of Information Photonics and Optical Communications, Beijing University of Posts and Telecommunications, Beijing 100876, China*
[2]*Department of Physics, University College Cork, Western Road, Cork, Ireland*
[3]*Tyndall National Institute, Lee Maltings, Cork, Ireland*
[4]*Center for Nanoscale Characterization and Devices, Wuhan National Laboratory for Optoelectronics, Huazhong University of Science and Technology, Wuhan 430074, China*

(Received 7 October 2016; accepted 25 January 2017; published online 6 February 2017)

Near-infrared nanowire lasers are promising as ultrasmall, low-consumption light emitters in on-chip optical communications and computing systems. Here, we report on a room-temperature near-infrared nanolaser based on an AlGaAs/GaAs nanowire/single-quantum-well heterostructure grown by Au-catalyzed metal organic chemical vapor deposition. When subjects to pulsed optical excitation, the nanowire exhibits lasing, with a low threshold of 600 W/cm^2, a narrow linewidth of 0.39 nm, and a high Q factor of 2000 at low temperature. Lasing is observed up to 300 K, with an ultrasmall temperature dependent wavelength shift of 0.045 nm/K. This work paves the way towards ultrasmall, low-consumption, and high-temperature-stability near-infrared nanolasers. *Published by AIP Publishing.* [http://dx.doi.org/10.1063/1.4975780]

Semiconductor nanowires (NWs) have been considered as excellent building blocks for future devices due to their unique geometry and superior electrical and optical properties.[1–3] Single NWs are particularly promising for compact nanolasers as they can provide both a gain medium and microcavity, which provide good optical feedback for lasing.[4–7] To date, room-temperature NW lasers have been achieved in various materials, involving ZnO, GaN, CdS, InP, and GaAs.[8–14] In comparison with homogeneous NWs, NW heterostructures incorporating quantum well (QW) or quantum dots (QDs) are expected to have distinct advantages for lasers such as low threshold, improved temperature stability, and wide-range wavelength tunability.[15–17] Moreover, radial NW/QW or NW/QD heterostructures decouple the gain medium and the optical cavity, avoiding the reabsorption of emission during its propagation in the NW cavity.[18] So far, radial NW/QW or NW/QD heterostructures have been fabricated in GaN/InGaN, InP/InAs, GaAs/In(Ga)As, and AlGaAs/GaAs.[17,19–24] Fabry-Pérot cavity modes have been widely observed in these structures, and room temperature lasing has also been achieved in some of them.[17,21–24] For example, individual GaN/InGaN multiple QW (MQW) NW has been reported to yield room-temperature composition-dependent lasing over a broad wavelength range, which is promising for wavelength-tunable sources.[17]

Since its birth in 1970, AlGaAs/GaAs double-heterostructure lasers have been widely used in optical communications and optical storage.[25] AlGaAs/GaAs NW heterostructure lasers are promising in short-range optical communications and chip-to-chip or on-chip optical interconnections. Recently, room-temperature AlGaAs/GaAs MQW NW lasers have been reported.[23,24] In comparison with the MQW NW, single QW (SQW) NW has a simpler structure and reduced dimension. In this work, we report on a low-threshold room-temperature laser based on a single AlGaAs/GaAs SQW NW grown by metal organic chemical vapor deposition (MOCVD). Low-temperature lasing was observed with a low threshold of 600 W/cm^2, a narrow linewidth of 0.39 nm, and a high Q factor of 2000. Lasing was observed up to 300 K, with an ultrasmall temperature dependent wavelength shift of 0.045 nm/K. The underlying lasing mechanism was theoretically investigated using the finite element method (FEM).

The AlGaAs/GaAs NW SQW heterostructures were grown by using a Thomas Swan closed coupled showerhead (CCS) MOCVD system at a pressure of 100 Torr. Trimethylgallium (TMGa), trimethylaluminum (TMAl), and arsine (AsH_3) were used as precursors. The carrier was hydrogen. An Au film with a thickness of 4 nm was deposited on the GaAs (111) B substrate by magnetron sputtering. The substrate was then loaded into the MOCVD reactor and annealed at 650 °C under AsH_3 ambient for 300 s to form catalyst. AlGaAs NWs were grown at 440 °C for 700 s. The flow rates of TMGa and TMAl were 39 and 18 μmol min^{-1}, respectively. After raising the temperature to 500 °C, a thin GaAs shell was radially grown on the AlGaAs NW for 150 s with a low TMGa flow rate of 5.4 μmol min^{-1}. Then, an AlGaAs shell was radially grown on the GaAs shell at 500 °C for 200 s, with a flow rate of 39 and 18 μmol min^{-1} for TMGa and TMAl, respectively. In the structure, the GaAs shell acts as the QW, while the AlGaAs core and shell function as the barriers.

The NWs were characterized by scanning electron microscopy (SEM), X-ray energy dispersive spectroscopy (EDS), and aberration corrected high-angle annular dark field/scanning transmission electron microscopy (HAADF/STEM). For HAADF/STEM studies, a thin NW slice is prepared by focused ion beam (FIB). For optical characterization, as-grown

[a)]X. Yan and W. Wei contributed equally to this work.
[b)]Electronic mail: xzhang@bupt.edu.cn

NWs were mechanically cut down and dispersed onto a Si/Ag/MgF_2 substrate. The substrate was fabricated by depositing a 200 nm Ag film on a Si substrate, followed by depositing a 5 nm MgF_2 film using electron beam evaporation. For lasing characterization, a home-built pulsed laser was used to pump the NW (a fiber laser providing 6 ps pulses at a wavelength of 532 nm with the repetition rate of 32 MHz). The excitation beam was focused onto ~2 μm in diameter with a ×50 microscope objective on the sample placed in a cryostat. The emission through the same microscope objective was detected by the combination of a grating spectrometer and a silicon charge-coupled device (CCD).

Fig. 1(a) shows the SEM image of the as-grown NW array. The NWs are vertical to the substrate with a diameter ranging from several dozen to several hundred nanometers. The inset shows an enlarged SEM image of the NW top. The different contrasts clearly demonstrate a core-shell structure. Fig. 1(b) shows the SEM image of a single lying NW, which has a length of approximately 8 μm and a uniform diameter of about 300 nm. The NW has a common hexagonal cross section, as shown in the inset. Fig. 1(c) shows the cross-sectional HAADF/STEM image. The QW can be clearly distinguished between the core and shell due to different brightness intensities. The core and shell contain an Al composition of 20% and 30%, respectively, according to the EDS results. The AlGaAs shell exhibits an inequilateral hexagonal cross-section and nonuniform thickness, which is attributed to an asymmetric lateral growth. The six sidewalls are {112} atomic planes with three of them belonging to $\{112\}_A$ and the other three belonging to $\{112\}_B$. As has been reported, the lateral growth on $\{112\}_A$ sidewalls is faster than that on $\{112\}_B$ sidewalls.[26] Fig. 1(d) shows the magnified HAADF/STEM image across a section of GaAs QW and AlGaAs barriers, revealing high-quality interface abruptness. The QW thickness (about 5 nm) is much smaller than the exciton Bohr radius in GaAs, which means that a strong quantum confinement effect could be expected in the structure.[27]

To investigate the lasing characteristics of single NWs, PL spectroscopy was performed under 532 nm pulsed laser excitation at 80 K. Fig. 2(a) shows the PL spectra with various excitation power densities. Above an excitation power density of ~600 W/cm^2, the peak at 781 nm increases sharply in intensity and its linewidth narrows, which is a signature of lasing. FEM simulations show that the NW can support three waveguide modes, HE_{11x}, HE_{11y}, and TE_{01}, while TE_{01} has the smallest threshold gain. According to the single mode lasing character in the experiment, the lasing mode is determined to be TE_{01}. Fig. 2(b) plots the double-logarithmic integrated light-out versus light-in (L–L) plot of the lasing peak at 781 nm, exhibiting an S-shaped nonlinear behavior, which is a characteristic of the transition from spontaneous to amplified spontaneous emission and finally lasing. We also observe a gradual narrowing of the linewidth from ~1.8 nm to ~0.4 nm when the excitation power density increases from 290 W/cm^2 to 2.9 kW/cm^2. At an excitation power density of 2.9 kW/cm^2, the laser exhibits a narrowest linewidth of 0.39 nm, as shown in Fig. 2(c). This corresponds to a high Q factor of 2000, which is much higher than the Q factors of GaAs/AlGaAs NW lasers.[12,28,29] The high Q factor could be attributed to the decoupling of the gain medium from the optical cavity, which dramatically reduces the absorption loss of emission in the cavity. When the excitation power further increases, the linewidth of the lasing peak turns to increase due to the phase fluctuations arising from

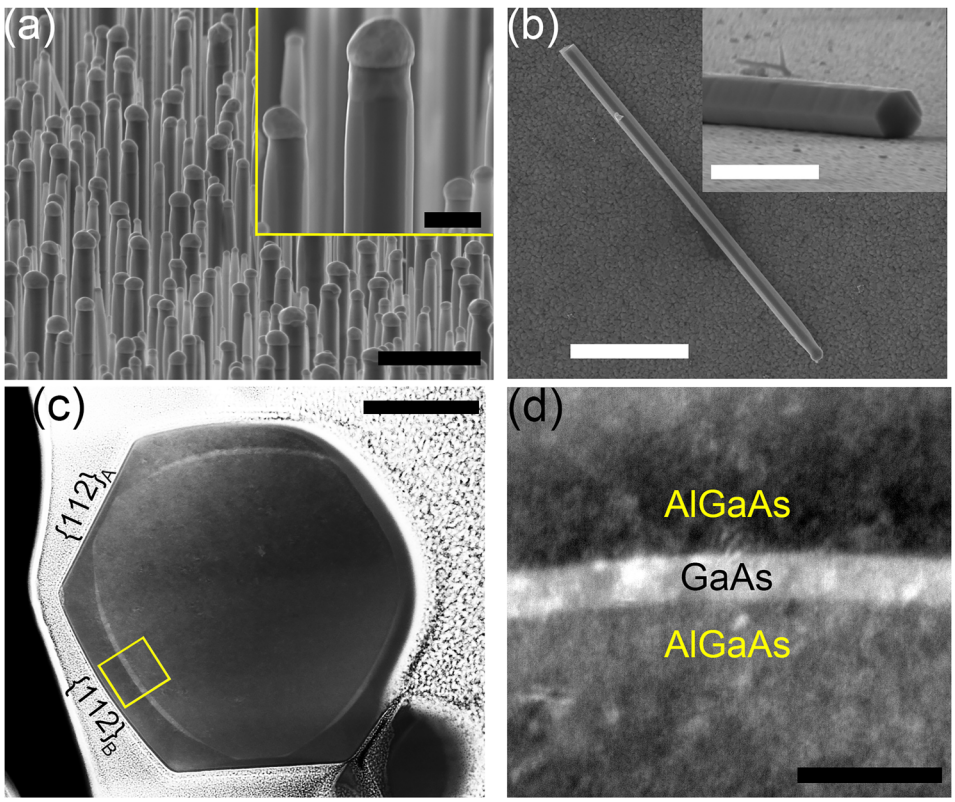

FIG. 1. (a) SEM image of the as-grown NW array. The inset shows an enlarged SEM image of the NW top. The scale bars in (a) and the inset are 1 μm and 200 nm, respectively. (b) Top-view SEM image of a single NW. The inset shows the lateral-view SEM image of a single NW. The scale bars in (a) and the inset are 2 μm and 1 μm, respectively. (c) Cross-sectional HAADF/STEM image of the NW. The scale bar is 100 nm. (d) Magnified HAADF/STEM image across a section of GaAs QW and AlGaAs barriers as indicated by the rectangular frame in (c). The scale bar is 10 nm.

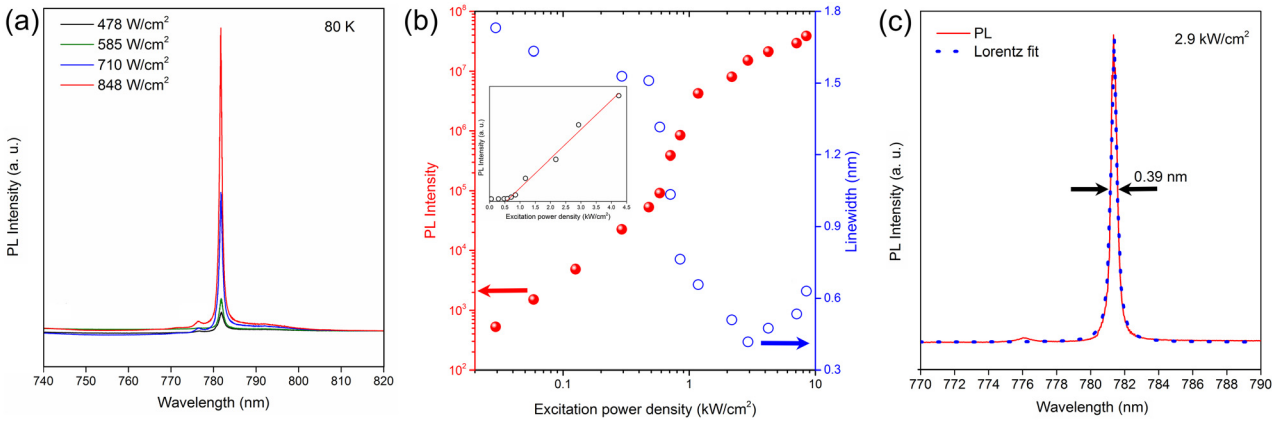

FIG. 2. Low-temperature lasing characteristics. (a) Emission spectra for a single NW at various excitation power density at 80 K. (b) Double-logarithmic integrated output-power intensities of the lasing peak with corresponding linewidth versus excitation power density. The inset shows the threshold knee behavior plotted on a linear scale. (c) The lasing spectra at 2.9 kW/cm^2, which has a narrow linewidth of 0.39 nm.

spontaneous emission events and their related refractive index perturbations, as well as the faster stimulated emission dynamics in the strong excitation regime.[30,31]

The lasing behavior can be observed up to room temperature. Fig. 3(a) presents the room-temperature PL spectra at different excitation power densities. With the increasing excitation power, a sudden increase in emission intensity is observed at 791 nm. Fig. 3(b) presents the double-logarithmic L-L plot, which shows an S-shaped behavior at a threshold power density of 2.5 kW/cm^2. The threshold for the laser at room temperature is about 4 times as large as that at 80 K, as higher carrier density is required to satisfy the threshold gain with increasing the temperature.[12] Fig. 3(c) shows the PL spectra of the same NW for temperature ranging from 80 to 300 K. It can be seen that lasing is obtained at all temperatures, while both the lasing wavelength and linewidth change with temperature. The dependence of the lasing wavelength and linewidth on temperature is presented in Fig. 3(d). With increasing temperature, the lasing peak exhibits a redshift of only 10 nm, much smaller than the bandgap reduction of GaAs, indicating that the temperature dependence of the laser emission wavelength is dominated by the variation of the refractive index in the case of NW cavity with a very small cavity length.[16,32] The wavelength

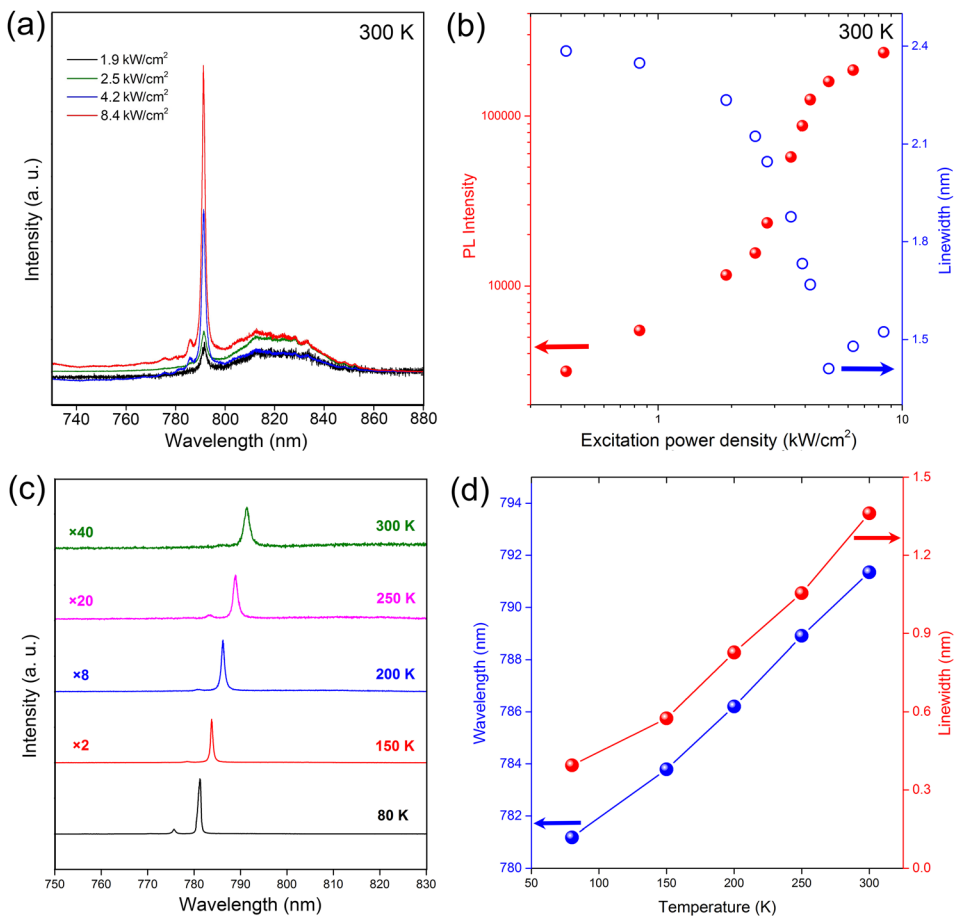

FIG. 3. Temperature dependence of the lasing characteristics. (a) Emission spectra for a single NW at various excitation power density at room temperature. (b) Double-logarithmic integrated output-power intensities of the lasing peak with corresponding linewidth versus excitation power density at room temperature. (c) Temperature dependence of the lasing spectra recorded above threshold at temperatures ranging from 80 to 300 K. (c) Dependence of the lasing wavelength and linewidth on temperature.

increases nearly linearly with a slope of 0.045 nm/K, much smaller than the QW and NW lasers, and even smaller than some QD lasers.[12,13,16,23,33–35] The high temperature stability of lasing wavelength makes the laser promising for uncooled device applications.[33] The linewidth increases from ~0.4 to ~1.4 nm as the temperature increases from 80 K to 300 K, which could be attributed to the faster variation of the gain in comparison with the refractive index, as well as the change of carrier concentration.[36]

In order to understand the underlying lasing mechanism, FEM simulations are carried out on an AlGaAs/GaAs SQW NW on top of both SiO_2 and Ag/MgF_2 substrates at room temperature, as illustrated in Fig. 4(a) and Fig. 4(b). For the NW on the SiO_2 substrate, partial pump energy is scattered without being absorbed by the NW to generate photons due to the transmission at the interface of NW/SiO_2 substrate. However, for the NW on the Ag/MgF_2 substrate, transmitted pump energy through the NW is highly reflected by the Ag film and reabsorbed by the NW. The optical absorption enhancement of the NW can be calculated by the ratio of integration of electric field intensity inside the NW cross-section of each system.[37] For an incident wavelength of 532 nm, the theoretical reflection enhancement is ~26×, which dramatically increases the optical absorption of the NW. Particularly, the Ag film can also enhance the optical absorption of the QW, which acts as the gain medium and dominates lasing. Under optical pump, the AlGaAs NW absorbs part of the pump energy and generates photons, which may scatter through the SiO_2 substrate. In the presence of the Ag film, most of the scattered photons can be reflected back into the NW and reabsorbed by the QW. Fig. 4(c) presents the room-temperature PL spectra of NW on SiO_2 and Ag/MgF_2 substrates, respectively. The PL intensity of the GaAs SQW on the Ag/MgF_2 substrate is nearly 10 times higher than that on the SiO_2 substrate, suggesting a much sufficient optical absorption, which contributes to the low-threshold lasing. It is necessary to point out that due to the presence of the metallic layer, the photons in the NW can excite surface plasmon polaritons forming the hybrid photon-plasmon mode. However, according to the results in Ref. 38, for a large NW diameter of around 300 nm, the mode is photonic-like mode. Thus for the SQW NW, photons make major contributions to lasing rather than plasmons.

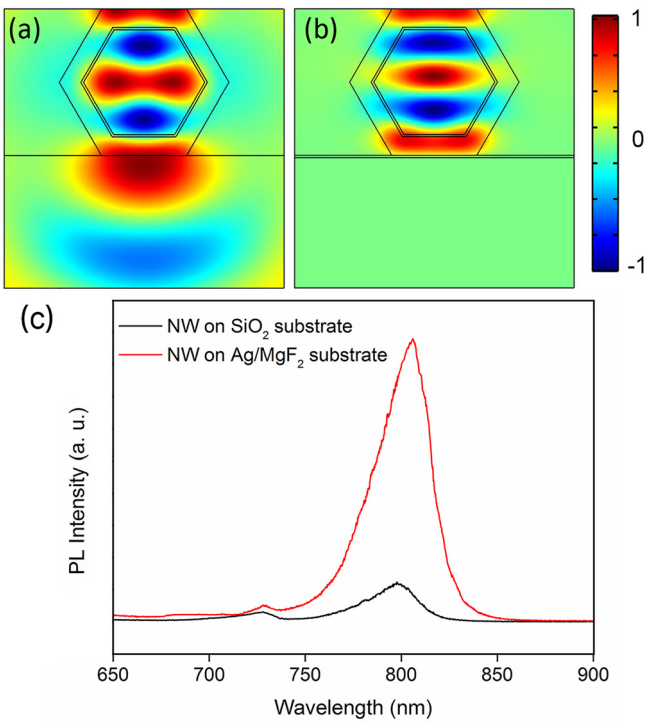

FIG. 4. (a) and (b) Transmission of electric field Ez in the NW on SiO_2 and Ag/MgF_2 substrates, respectively. (c) Room-temperature PL spectra of NW on SiO_2 and Ag/MgF_2 substrates, respectively. The NW is pumped with a continuous-wave 532 nm laser at a power density of 630 W/cm^2.

In summary, we have demonstrated a low-threshold room-temperature near-infrared nanolaser based on an AlGaAs/GaAs SQW NW grown by MOCVD. When subjects to pulsed optical excitation, the NW exhibits lasing with a low threshold of 600 W/cm^2, a narrow linewidth of 0.39 nm, and a high Q factor of 2000. Lasing is observed up to 300 K, with an ultrasmall temperature dependent wavelength shift of 0.045 nm/K, even smaller than some QD lasers, suggesting the high-thermal-stability of the laser. FEM simulations demonstrate that the lasing mode is the TE_{01} mode, and the low-threshold could be majorly attributed to the enhancement of the optical absorption by the highly reflective metal substrate. The threshold may be further reduced by incorporating MQW heterostructures, and lasing wavelength can also be tuned by adjusting the QW thickness and composition. Our demonstration is a major step towards the future realization of NW lasers utilizing QWs with low-consumption, high-temperature-stability, and wide-range wavelength tunability.

This work was supported by the National Natural Science Foundation of China (61504010, 61376019, and 61511130045), the European Office of Aerospace Research and Development (FA9550-14-1-0204), the Science Foundation Ireland (12/IP/1658), Beijing Natural Science Foundation (4142038), and the Fund of State Key Laboratory of Information Photonics and Optical Communications (Beijing University of Posts and Telecommunications), P. R. China.

[1]Y. Li, F. Qian, J. Xiang, and C. M. Lieber, Mater. Today **9**, 18 (2006).
[2]P. J. Pauzauskie and P. Yang, Mater. Today **9**, 36 (2006).
[3]F. Patolsky, B. P. Timko, G. Zheng, and C. M. Lieber, MRS Bull. **32**, 142 (2007).
[4]C. Couteau, A. Larrue, C. Wilhelm, and C. Soci, Nanophotonics **4**, 90 (2015).
[5]B. Hua, J. Motohisa, Y. Ding, S. Hara, and T. Fukui, Appl. Phys. Lett. **91**, 131112 (2007).
[6]Y. Ding, J. Motohisa, B. Hua, S. Hara, and T. Fukui, Nano Lett. **7**, 3598 (2007).
[7]M.-K. Seo, J.-K. Yang, K.-Y. Jeong, H.-G. Park, F. Qian, H.-S. Ee, Y.-S. No, and Y.-H. Lee, Nano Lett. **8**, 4534 (2008).
[8]M. H. Huang, S. Mao, H. Feick, H. Yan, Y. Wu, H. Kind, E. Weber, R. Russo, and P. Yang, Science **292**, 1897 (2001).
[9]S. Liu, C. Li, J. J. Figiel, S. R. J. Brueck, I. Brener, and G. T. Wang, Nanoscale **7**, 9581 (2015).
[10]S. Geburt, A. Thielmann, R. Röder, C. Borschel, A. McDonnell, M. Kozlik, J. Kühnel, K. A. Sunter, F. Capasso, and C. Ronning, Nanotechnology **23**, 365204 (2012).
[11]Q. Gao, D. Saxena, F. Wang, L. Fu, S. Mokkapati, Y. Guo, L. Li, J. Wong-Leung, P. Caroff, H. H. Tan, and C. Jagadish, Nano Lett. **14**, 5206 (2014).
[12]D. Saxena, S. Mokkapati, P. Parkinson, N. Jiang, Q. Gao, H. H. Tan, and C. Jagadish, Nat. Photonics **7**, 963 (2013).

[13]B. Mayer, D. Rudolph, J. Schnell, S. Morkötter, J. Winnerl, J. Treu, K. Müller, G. Bracher, G. Abstreiter, G. Koblmüller, and J. J. Finley, Nat. Commun. **4**, 2931 (2013).
[14]W. Wei, Y. Liu, X. Zhang, Z. Wang, and X. Ren, Appl. Phys. Lett. **104**, 223103 (2014).
[15]Y. Arakawa and H. Sakaki, Appl. Phys. Lett. **40**, 939 (1982).
[16]J. Tatebayashi, S. Kako, J. Ho, Y. Ota, S. Iwamoto, and Y. Arakawa, Nat. Photonics **9**, 501 (2015).
[17]F. Qian, Y. Li, S. Gradečak, H.-G. Park, Y. Dong, Y. Ding, Z. L. Wang, and C. M. Lieber, Nat. Mater. **7**, 701 (2008).
[18]M. Moewe, L. C. Chuang, S. Crankshaw, K. W. Ng, and C. Chang-Hasnain, Opt. Express **17**, 7831 (2009).
[19]P. Mohan, J. Motohisa, and T. Fukui, Appl. Phys. Lett. **88**, 133105 (2006).
[20]X. Yan, X. Zhang, J. Li, Y. Wu, B. Li, and X. Ren, Phys. Status Solidi-R **10**, 168 (2016).
[21]X. Yan, X. Zhang, J. Li, Y. Wu, J. Cui, and X. Ren, Nanoscale **7**, 1110 (2015).
[22]X. Yan, X. Zhang, X. Ren, X. Lv, J. Li, Q. Wang, S. Cai, and Y. Huang, Nano Lett. **12**, 1851 (2012).
[23]T. Stettner, P. Zimmermann, B. Loitsch, M. Döblinger, A. Regler, B. Mayer, J. Winnerl, S. Matich, H. Riedl, M. Kaniber, G. Abstreiter, G. Koblmüller, and J. J. Finley, Appl. Phys. Lett. **108**, 011108 (2016).
[24]D. Saxena, N. Jiang, X. Yuan, S. Mokkapati, Y. Guo, H. H. Tan, and C. Jagadish, Nano Lett. **16**, 5080 (2016).
[25]Z. I. Alferov, V. M. Andreev, E. L. Portnoi, and M. K. Trukan, "AlAs-GaAs heterojunction injunction lasers with a low room-temperature threshold," Sov. Phys. Semicond. **3**, 1107 (1970).
[26]J. Zou, M. Paladugu, H. Wang, G. J. Auchterlonie, Y.-N. Guo, Y. Kim, Q. Gao, H. J. Joyce, H. H. Tan, and C. Jagadish, Small **3**, 389 (2007).
[27]R. C. Miller, D. A. Kleinman, W. T. Tsang, and A. C. Gossard, Phys. Rev. B **24**, 1134 (1981).
[28]B. Hua, J. Motohisa, Y. Kobayashi, S. Hara, and T. Fukui, Nano Lett. **9**, 112 (2009).
[29]W. Wei, X. Zhang, X. Yan, and X. Ren, AIP Adv. **5**, 087148 (2015).
[30]D. Welford and A. Mooradian, Appl. Phys. Lett. **40**, 865 (1982).
[31]B. Mayer, L. Janker, B. Loitsch, J. Treu, T. Kostenbader, S. Lichtmannecker, T. Reichert, S. Morkötter, M. Kaniber, G. Abstreiter, C. Gies, G. Koblmüer, and J. J. Finley, Nano Lett. **16**, 152 (2016).
[32]J. Talghader and J. S. Smith, Appl. Phys. Lett. **66**, 335 (1995).
[33]F. Schäfer, J. P. Reithmaier, and A. Forchel, Appl. Phys. Lett. **74**, 2915 (1999).
[34]R. Schwertberger, D. Gold, J. P. Reithmaier, and A. Forchel, IEEE Photonic. Tech. L. **14**, 735 (2002).
[35]F. Klopf, S. Deubert, J. P. Reithmaier, and A. Forchel, Appl. Phys. Lett. **81**, 217 (2002).
[36]M. Osiński and J. Buus, IEEE J. Quantum Elect. **23**, 9 (1987).
[37]S. Arab, P. D. Anderson, M. Yao, C. Zhou, P. D. Dapkus, M. L. Povinelli, and S. B. Cronin, Nano Res. **7**, 1146 (2014).
[38]R. F. Oulton, V. J. Sorger, D. A. Genov, D. F. P. Pile, and X. Zhang, Nat. Photonics **2**, 496 (2008).